Polish Society of Composite Materials
Polskie Towarzystwo Materiałów Kompozytowych

12: 4 (2012) 237-244

COMPOSITES THEORY AND PRACTICE

Andrzej Leski[1], Mariusz Wesołowski[2], Michał Stefaniuk[1]*

[1]Air Force Institute of Technology, Division for Reliability & Safety of Aeronautical Systems, ul. Księcia Bolesława 6, 01-494 Warszawa, Poland
[2]Air Force Institute of Technology, Division for Airfield Systems, ul. Księcia Bolesława 6, 01-494 Warszawa, Poland
**Corresponding author. E-mail: michal.stefaniuk@itwl.pl*

Received (Otrzymano) 20.01.2012

EVALUATION OF MOBILE, COMPOSITE AIRFIELD MAT

One of the basic requirements needed for proper aircraft operation in combat situations is the provision of an adequate number of airfields and a sufficient level of operational readiness. The rapid repair of airfield pavements enables quick resumption of air operations. The existing technology and methods of airfield pavement reconstruction could not meet the stringent time requirements of military operations, that is why mobile, composite airfield mats have been developed. In the paper, the operational and maintenance advantages of the elastic, mobile airfield mat ELP-1 KRATER manufactured by Stocznia Żuławy Sp. z o.o. are shown. The results of field and laboratory tests, performed by the Air Force Institute of Technology, Poland (ITWL) are also shown. The laboratory tests consisted of basic material property testing, as well as fatigue testing of the composite material. Strength tests of the mat-to-ground anchoring bolts were also performed, the results of which are presented in the paper. The field tests consisted of two stages: static and dynamic. In the static tests, the quality of the crater soil filling was tested with pressure plates and deflectometers. The dynamic testing had the form of several runs with a heavy truck on the mat-subbase system instrumented with strain gauges. These braking runs were an approximation of the loading conditions present during aircraft landing, and the weight of the test vehicle was comparable to the weight of transport aircraft. The overall levels of the recorded reaction forces were low, and the heaviest loading occurred during the most aggressive braking and turning maneuvers. The preliminary numerical model of the system consisting of the mat and the soil subbase is also presented. The numerical analysis was performed with the use of the Finite Element Method (FEM). A local model used to test the subbase stiffness was created alongside an associated global model which was employed to simulate the heavy test vehicle runs. The FE analysis has confirmed the theoretical assumptions and helped to put the experimental results in a proper framework. The overall evaluation proves that the mechanical strength of the composite mats is sufficient to withstand loads that may come from heavy military aircraft.

Keywords: mobile airfield mats, runway damage repair, composite mat, finite element method

BADANIA MOBILNEGO, KOMPOZYTOWEGO POKRYCIA LOTNISKOWEGO

Jednym z głównych wymagań niezbędnych do poprawnego prowadzenia operacji powietrzach w sytuacjach bojowych jest posiadanie dostatecznej liczby lotnisk i odpowiedniego poziomu gotowości operacyjnej. Szybka naprawa nawierzchni lotniskowej pozwala na szybkie wznowienie działań powietrznych. Istniejąca technologia i metody rekonstrukcji nawierzchni lotniskowych nie sprostały wysokim wymaganiom czasowym istniejącym w sytuacjach bojowych. Z tego powodu wynaleziono mobilne, kompozytowe pokrycia lotniskowe. W niniejszym artykule ukazano zalety wykorzystywania elastycznego, mobilnego pokrycia ELP-1 KRATER, wyprodukowanego przez Stocznię Żuławy Sp. z o.o. Zaprezentowano również wyniki badań laboratoryjnych i poligonowych przeprowadzonych przez Instytut Techniczny Wojsk Lotniczych. Badania laboratoryjne opierały się na badaniach własności materiałowych oraz na badaniach zmęczeniowych materiału kompozytowego, wykonano także badania wytrzymałościowe śrub kotwiących - wyniki przedstawiono w artykule. Badania poligonowe zawierały dwa etapy: statyczny i dynamiczny. Podczas testów statycznych jakość wypełnienia uszkodzenia typu krater została przebadana za pomocą płyt dynamicznych oraz ugięciomierzy. Testy dynamiczne polegały na wielu przejazdach obciążonym samochodem ciężarowym po układzie podłoże-pokrycie i pomiarze tensometrycznym obciążeń. Gwałtowne hamowania samochodu miały odpowiadać warunkom obciążenia panującym podczas lądowania samolotu, a ciężar samochodu był porównywalny z ciężarem samolotu transportowego. Zmierzone wartości sił reakcji były niewielkie, największe wartości osiągając podczas najbardziej gwałtownych manewrów skrętu i hamowania. W artykule przedstawiono także wstępny numeryczny model układu podłoże-pokrycie. Do analizy modelu wykorzystano metodę elementów skończonych. Do analizy sztywności podłoża wykorzystano lokalny model, do analizy warunków testów dynamicznych wykorzystano model globalny. Wyniki symulacji potwierdziły założenia teoretyczne oraz pozwoliły poprawnie zinterpretować wyniki badań terenowych. Wyniki badań i analiz wskazały, iż wytrzymałość pokrycia jest wystarczająca do przeniesienia obciążeń pochodzących od ciężkich samolotów wojskowych.

Słowa kluczowe: mobilne pokrycia lotniskowe, naprawy nawierzchni lotniskowych, maty kompozytowe, metoda elementów skończonych

INTRODUCTION

The mobile, composite airfield mat ELP-1 KRATER is manufactured in Poland by Stocznia Żuławy sp. z o.o. The design works started in 1999. The design goal was to use the mat as a means to repair airfields damaged due to directed enemy action [1, 2], or as a temporary helipad (e.g. near field hospitals) or as

a way to repair roads that have particular, military significance. After the acceptance procedures were completed, in 2002 the production of the mats was launched, and in 2008 the product was introduced into service in the Polish military.

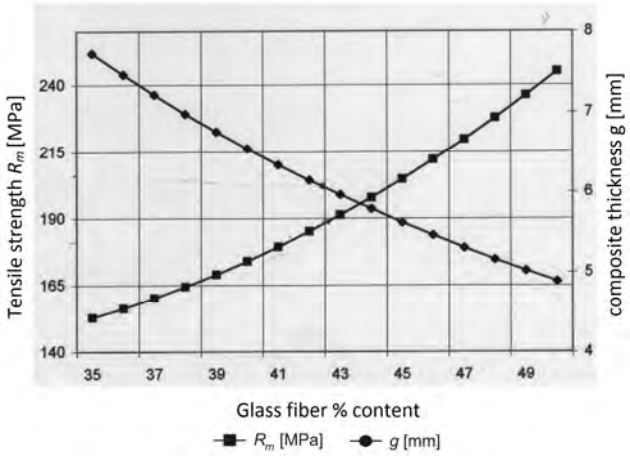

Fig. 1. Relation between glass fiber content and tensile strength of composite

Rys. 1. Zależność pomiędzy zawartością włókna szklanego a wytrzymałością kompozytu

Polyester resin (type PALATAL U 541) serves as the matrix in the composite material, and E - type glass fiber from the Krosno Glassworks serves as the reinforcement. Glass fiber constitutes 44% of the composite volume. The optimal percentage of glass fiber was chosen according to Figure 1. The composite used has the parameters listed in Table 1, the manufacturer-provided data is presented in Table 2. The ELP-1 KRATER air field mat consists of 9 elements (1.8 m wide; 9.1 m long and 8 mm thick). The elements are connected with elastic joints that facilitate cooperation of the segments. An assembly of 9 segments constitutes a half-mat, and two are connected together to form a complete 16.8 x 18.2 m airfield mat. The elastic joint segment is made of five layers of polyester woven fabric, bonded on both sides with polyurethane. The width of the connectors is 70 cm. The layers are interwoven with glass-fiber reinforcement. The final composite set-up consists of ten plies of glass fiber and two layers of weave [3]. In Figures 2 and 3 the whole mat system is shown.

TABLE 1. **Composite properties**
TABELA 1. **Właściwości kompozytu**

Resin percentage	45.00%
Reinforcement mass	5.00 kg/m^2
Resin mass	6.11 kg/m^2
Laminate mass	11.11 kg/m^2
Single segment weight	182.00 kg
Cover weight	1 638.00 kg
Mat weight	3 276.00 kg
Mat area	150.15 m^2

TABLE 2. **Manufacturer material data**
TABELA 2. **Dane producenta**

Extensional strength	145 MPa
Bending strength	205 MPa
Tensile modulus	12 100 MPa
Bending modulus	8 950 MPa

The mats were manufactured on specialized rigs. Each mat segment was overlapped with an elastic connector panel. To obtain the highest possible mechanical properties, measures were taken to ensure uniformity of the material structure. In the manufacturing stage, the mechanical properties of the composite were determined based on the known properties of the individual layers, which enabled predictive calculations of the final product mechanical characteristics [4]. The resulting composite material had to meet the specified technical criteria - most importantly the ability to withstand static, dynamic and thermal loads coming from the aircraft that traverse the airfield mat. A mobile composite mat must also be resistant to aggressive chemical agents which act on the structure in the operational environment. Therefore there was a need to test the properties in a laboratory setting.

Fig. 2. Method of connecting of mat segments

Rys. 2. Sposób łączenia elementów maty

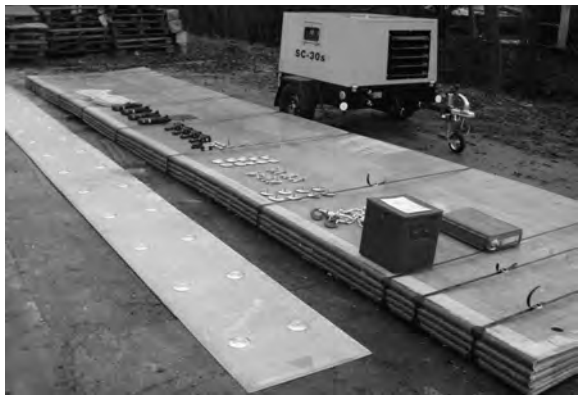

Fig. 3. Airfield mat in transport configuration

Rys. 3. Mata lotniskowa w konfiguracji transportowej

LABORATORY TESTING

Fatigue testing of composite specimens

The airfield mats have been subjected to a series of material tests (tension test, fatigue testing, fire-resis-

tance, anchoring strength tests etc.). In the present paper the results of bending fatigue testing and anchoring test results are presented.

Rectangular 250x25 mm specimens taken from a manufactured mat were used for the fatigue tests in two orthogonal directions - parallel and perpendicular to the fibers [5]. Three-point bending test series were performed, with a defined number of cycles for each of the series, with constant displacement of the middle portion of the specimen. The fatigue test frequency was 2 Hz, ambient temperature - 20 to 23°C and humidity 45-55%. In the tests, an initial deflection of 3 mm was introduced.

The recorded load levels (vs. number of load-cycles are presented in Figure 4 (parallel to fibers) and in Figure 5 (perpendicular to fibers).

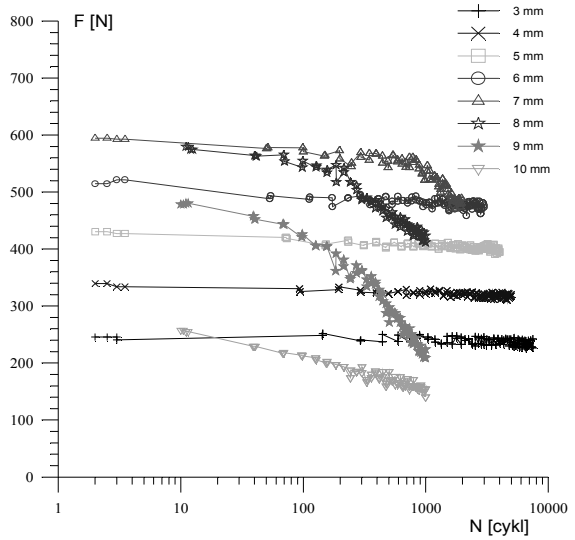

Fig. 4. Bending force vs. number of cycles for different load levels, lateral direction

Rys. 4. Siła zginająca w funkcji liczby cykli dla różnych poziomów obciążenia, kierunek wzdłużny

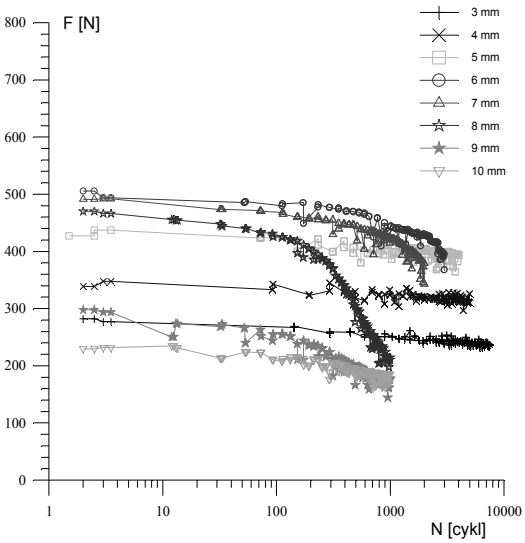

Fig. 5. Bending force vs. number of cycles for different load levels, transverse direction

Rys. 5. Siła zginająca w funkcji liczby cykli dla różnych poziomów obciążenia, kierunek poprzeczny

TABLE 3. **Fatigue test program**
TABELA 3. **Program testowy zmęczenia**

Deflection [mm]	Number of cycles			
	Lateral direction		Transverse direction	
	Specimen 1	Specimen 2	Specimen 1	Specimen 2
3	15000	7500	7500	7500
4		5000	5000	5000
5	7500	4000	4000	4000
6		3000	3000	3000
7	1000+1000	2000	2000	2000
8		1000	1000	1000
9	1000+1000	1000	1000	1000
10		1000	1000	1000

Table 3 shows the test program in detail. For each case, the load level was different. For a high number of cycles, a decrease in bending force could be seen that was more rapid at greater deflection levels. Sometimes, stepping in the load level could be seen, marking the onset of cracking. In the initial stage of the tests, for lower deflections, an increase in deflection caused an increase in exciting (bending) load, but after the crack was initiated, lower load increases were needed for a similar deflection increase. This was equivalent to a decrease in the material strength.

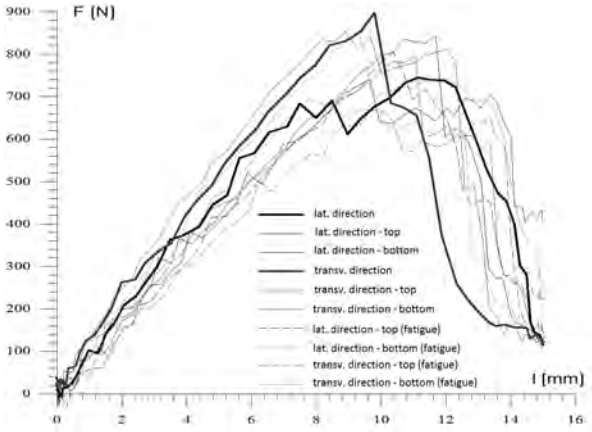

Fig. 6. Bending force vs. specimen deflection, conducted before (continuous lines), and after (dashed lines) fatigue testing

Rys. 6. Siła zginająca w funkcji ugięcia próbki, przed (linia ciągła) i po (linia przerywana) badaniach zmęczeniowych

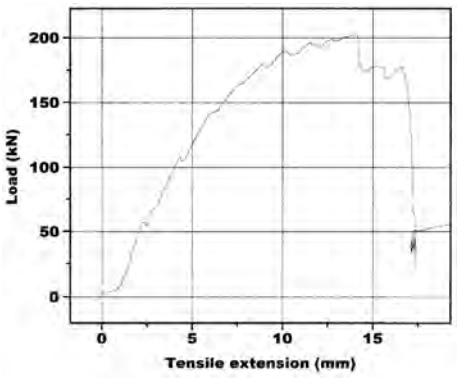

Fig. 7. Relation between tensile extension of segment and load

Rys. 7. Zależność między rozciągnięciem segmentu i obciążeniem

Mat to surface anchoring testing

Anchoring tests were performed to determine the strength of the bolted joints and to confirm that proper configuration of the bolting/anchors was chosen for the mat system. Pure shear was introduced to the testing, for which the strength of the joints and the nearby mat regions was determined. Figure 8 shows the testing method and Table 4 presents the displacement and load levels. Graphical illustration of the bending test is shown in Figure 6, the tension results can be seen in Figure 7. Laboratory verification testing has shown the joint strength to be adequate.

Fig. 8. Strength test of anchoring bolts
Rys. 8. Badanie wytrzymałości kotwienia

TABLE 4. **Measured displacements and loads**
TABELA 4. **Zmierzone odchyłki i obciążenia**

Specimen number	Force [kN]	Displacement [mm]
1	159.00	14.80
2	160.30	15.26
3	202.40	13.94
Mean:	173.90	14.67

FIELD TESTING

The field tests were carried out in three stages. In stage I, verification of crater-type pavement damage repair was carried out (i.e. quality of crater filling was checked). In stage II, the static load bearing capacity of the system consisting of the airfield mat along with the newly formed subbase was tested. Stage III consisted of dynamic tests of the mat-subbase system. The forces and displacements were measured with the use of a strain-gauge set, which enabled us to determine the composite mat system deflections, reaction forces in anchoring bolts, and of the forces acting between the mat-system segments.

Subbase tests

Acceptance tests of a newly formed Ground subbase [7] (essentially filling of large crater-type damage) have been carried out using a light dynamic plate HMP LFG-K, VSS equipment and a heavy impact deflectometer (type HWD). The crater dimensions were as follows: depth - 2.5 m, visible crater diameter - 6.4 m, and effective crater diameter - 11.8 m. The crater schematics are shown in Figure 9.

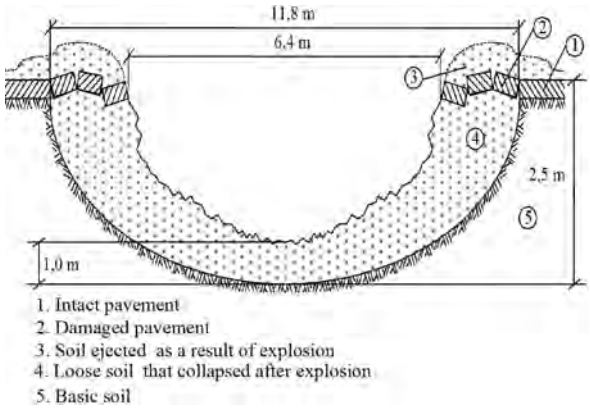

Fig. 9. Structure of crater-type damage
Rys. 9. Struktura uszkodzenia typu krater

A light dynamic plate was used to test the uniformity of the newly formed filling, and to determine the dynamic modulus E_{vd}. The measurements were taken at 9 test points (3 rows of 3 points). The results are shown in Table 5. Based on the calibration tests of other subbase materials, the relation between the static (VSS equipment) and dynamic (LDP) tests can be shown to be as follows:

$$E_{st} = E_{vd} \cdot 1.95 \tag{1}$$

TABLE 5. **Light dynamic plate test results**
TABELA 5. **Rezultaty testów lekkich dynamicznych płyt**

Measurement number	Dynamic modulus E_{vd} [MPa]	Static modulus E_{st} [MPa]
1	51.6	100.6
2	94.5	184.3
3	74.7	145.7
4	64.7	126.2
5	80.9	157.8
6	54.1	105.5
8	109.8	214.1
9	101.8	198.5
Mean value:	84.9	165.6

The static moduli values determined with this relation are listed in Table 5. A cross check of the load bearing capacity of the subbase was performed with the use of VSS. In this method, the displacement modulus is calculated, which is a measurement of the subbase bearing capacity. The modulus E is the ratio of the unit load increase to the displacement increase of the tested layer, for a specified range of unit load levels, multiplied by the loading plate diameter. Then numerical values are obtained with the formula:

$$E = \frac{3 \cdot \Delta p}{4 \cdot \Delta s} \cdot D \tag{2}$$

where: Δp - unit load increase for given range, Δs - displacement increase for specified load range (0.15÷0.25 MPa), loading plate diameter.

The tests were carried out according to standards BN-64/8931-02 and PN-S-02205:1998. The tests results are given in Table 6.

TABLE 6. **VSS test results**
TABELA 6. **Wyniki testów VSS**

Pressure Δp [MPa]	Mean measured displacement Δs [mm]			Mean Δs value [mm]
	I sensor	II sensor	III sensor	
0.00	0.00	0.00	0.00	
0.05	0.02	0.15	0.26	
0.15	0.33	0.58	1.15	0.68
0.25	0.53	0.85	1.75	1.04
0.35	0.69	1.06	2.20	
0.25	0.67	1.05	2.17	
0.15	0,67	1.01	2.11	
0.05	0.61	0.85	1.91	
0.00	0.31	0.60	1.71	
0.05	0.31	0.66	1.79	
0.15	0.39	0.84	2.06	1.09
0.25	0.46	0.98	2.31	1.25

The VSS testing method is illustrated in Figure 10. Relation (2) was used to determine the subbase (filling) displacement moduli: primary and secondary. The moduli values were measured to be as follows: E_1 = = 62.5 MPa, E_2 = 140.0 MPa. The moduli values are used to determine the subbase deflection coefficient I_0:

$$I_0 = \frac{E_2}{E_1} = \frac{140.0}{62.5} = 2.2 \tag{3}$$

The measured deflection-based displacement moduli values proved the density of the crater filling to be adequate. The subbase bearing capacity tests performed with the HWD deflectometer (Fig. 11) show good correlation with the VSS and LDP results. The subbase displacement modulus was calculated (3) to be 161.0 MPa.

$$E_0(0) = \frac{2 \cdot (1 - \nu^2) \cdot q \cdot a}{u(0)} \tag{4}$$

where: $E_0(0)$ - area modulus under plate; a - loading plate radius (150 mm); ν - Poisson ratio; u - deflection at measured point (0 - under plate); q - stress under plate.

Fig. 10. Displacement modulus tests with use of VSS
Rys. 10. Badanie modułu ugięcia przy pomocy VSS

Fig. 11. Bearing capacity tests with use of HWD
Rys. 11. Badania nośności przy pomocy HWD

Load carrying capacity tests

The mat-subbase system test has been carried out with a HWD deflectometer, a device used to measure the elastic deflections caused by a dynamic load [8, 9]. In the HWD method, a certain load is dropped on a damped pressure plate that lies on the tested surface. In the instant of the drop, transducers (geophones) mounted on the beam and under the plate itself, measure the deflection and its change in time. The elastic moduli of the individual layers of the subbase are computed with the use of (3). Subsequently, an iterational comparison of the theoretical and measured values is performed in such a way that function F is minimized:

$$F = \sum_{j=1}^{k} (w_j - u_j)^2 \tag{5}$$

where: w_j - calculated deflection at distance r from plate center; u_j - measured deflection at distance r from plate center; k - number of transducers.

Based on the deflection test results of the ELP-1 KRATER composite mat installed on the newly formed subbase filling, the relation between deflection w and subbase stiffness k has been obtained (Fig. 12). This plot shows that the use of a composite mat causes a decrease in deflection for the complete/whole mat-subbase structure, and therefore leads to a bearing capacity increase. The extent of the deflection decrease is linked to the bearing capacity of the subbase itself (expressed by stiffness coefficient k). For $k <$ 70 MN/m^3 (soil subbase with low bearing capacity), the ELP-1 KRATER has significant participation in load bearing and transfer; however, for $k \geq 70$ MN/m^3 (soil subbase of medium and high bearing capacity) the mat's contribution is very limited.

Dynamic testing

The main operational parameter for a mobile composite airfield mat is its load bearing capacity. Therefore, detailed analysis of the mat's working conditions was performed, and its aim was to determine the mat's participation in the transfer of loads caused by landing aircraft and maneuvering vehicles. The analysis results can be employed to determine which types of aircraft will be allowed to use the mat for landing, take off and associated maneuvers. During the field tests, the mat-

subbase system has been subjected to a dynamic load. The number of load variants was evaluated in which a heavily-laden vehicle (a truck) traversed the mat at different velocities and angles. The schematics of the measurement system are presented in Figure 13.

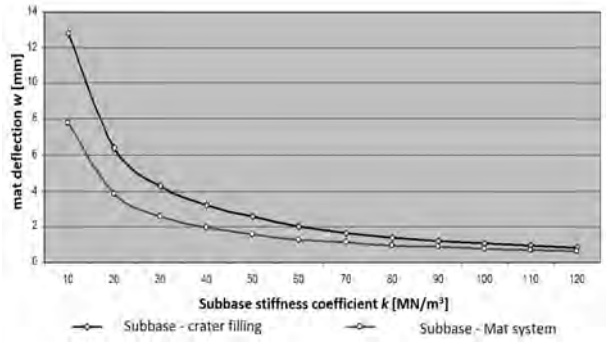

Fig. 12. Mat deflection as function of subbase stiffness coefficient

Rys. 12. Ugięcie maty w funkcji sztywności podłoża

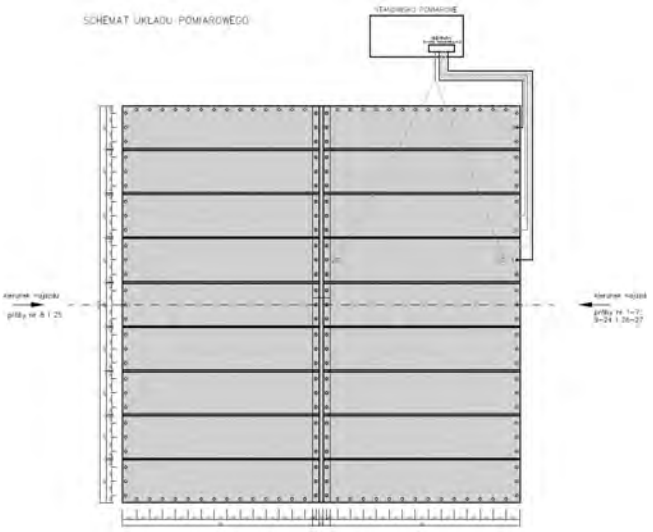

Fig. 13. Measurement system schematics

Rys. 13. Schemat układu pomiarowego

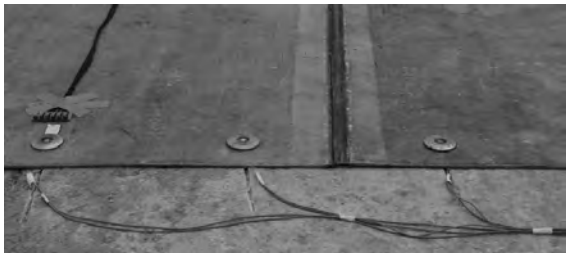

Fig. 14. Strain gauge placement on anchoring bolts

Rys. 14. Umiejscowienie tensometrów w obszarze kotwienia

Figure 15 shows the strain gauge system installed on ELP-1 KRATER. The truck made in total 27 passages at different speeds and with different loads. In testing, the strain gauges mounted to 5 bolts (Fig. 14) registered the actual in-plane forces in the anchoring region, i.e. two force components - parallel and perpendicular to the passage direction. Furthermore, the readings from strain gauges installed on the top surface of the composite mat were used to determine the actual displacements in the tested systems. An example of the force values recorded in one of the test sessions is presented in Figure 16. The passage is illustrated in Figure 17.

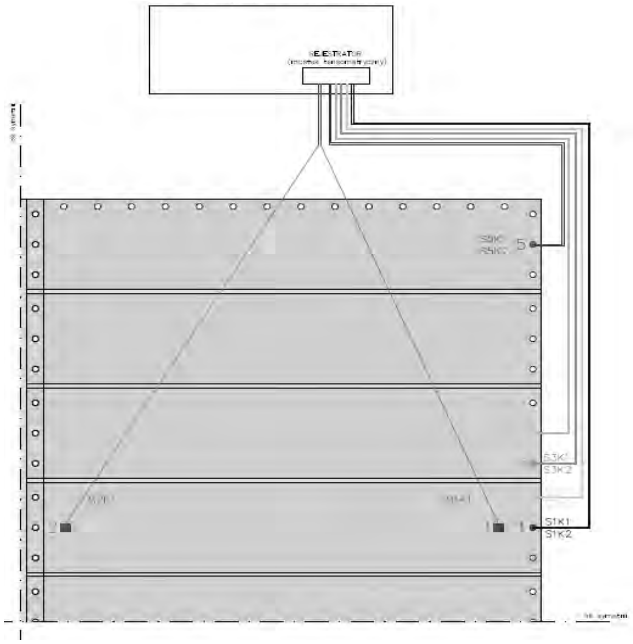

Fig. 15. Strain gauge placement on mat

Rys. 15. Umiejscowienie tensometrów na macie

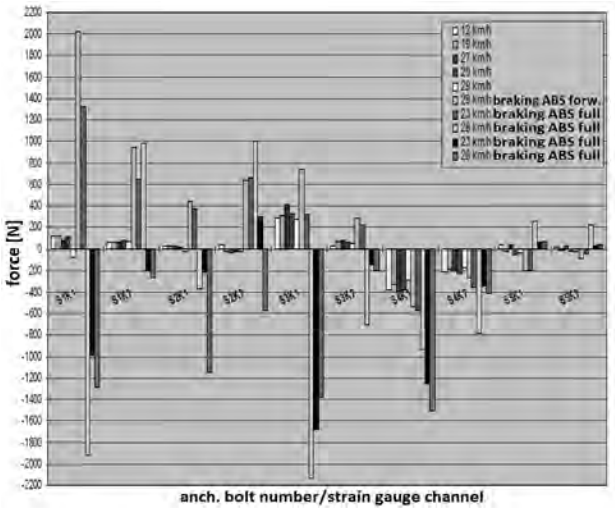

Fig. 16. Measured bolt reaction forces

Rys. 16. Zmierzone siły reakcji w obszarze kotwienia

Fig. 17. Vehicle braking during tests

Rys. 17. Hamowanie pojazdu podczas badań

NUMERICAL MODEL

The system consisting of the mobile airfield mat and the soil subbase has been modeled using numerical methods. Along with the analytical models [11], the numerical models currently used mainly utilize specialized tools and codes based on the Finite Element Method [12, 13]. In the present paper, universal, commercially available FEM codes were employed for the analysis. MSC PATRAN was used to create the FEM mesh, and to present the results. The numerical computations were performed using the MSC.MARC solver. The composite cover segments and the connection joints were modeled with thin shell elements. A linear elastic material was used, with the properties described with the Elastic modulus (120 GPa) and Poisson's ratio (0.288). The heavy truck field test loading was verified in the simulation, and the corresponding stresses and reaction forces were obtained. The global FEM model is shown in Figure 18.

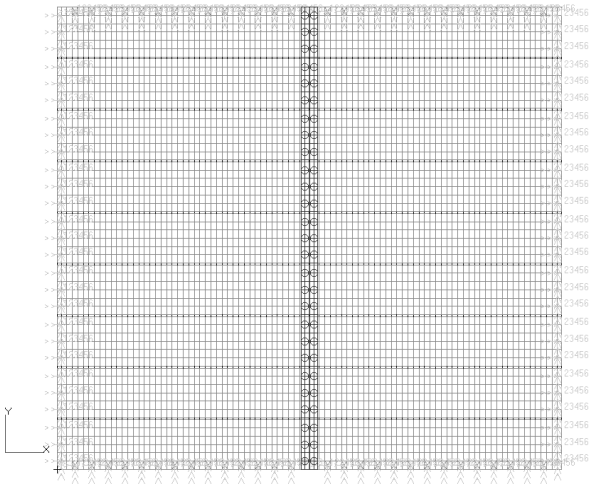

Fig. 18. Global finite element model of the airfield mat
Rys. 18. Globalny model numeryczny maty lotniskowej

For load bearing capacity (subbase stiffness) calibration, a local model of a 1 m x 1 m segment of the mat-subbase system has been implemented. An equivalent aircraft landing gear load has been applied to the modeled airfield mat surface. The densely meshed local model enabled the assessment of displacements in the surface normal (vertical) direction - i.e. a simulation of pressure plate tests (Fig. 19). In Figure 20, the calculated deflections and their comparison to the test results are plotted as a function of the subbase stiffness. The subbase was modeled as a set of discrete springs connected to each of the mat nodes with a "sliding surface" constraint to enable relative movement between the mat and the subbase, with stiffnesses determined through calibration. The local simulation results show that the main loading mode that leads to the airfield mat failure (esp. in the anchoring region) are due to in-plane forces acting on the surface. Such loads result from friction forces present under braking. In the dynamic field tests, runs with a 46-ton truck were performed at different velocities. In the numerical simulation, the dynamic braking load variant was approximated with the static tangential forces in the plane of the mat. These applied forces symbolize the friction between the composite mat and the vehicle tires.

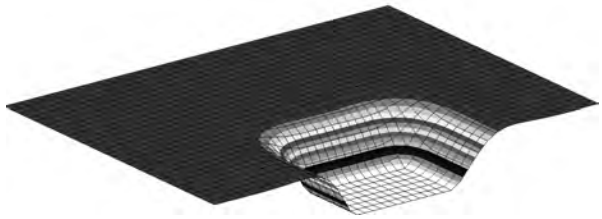

Fig. 19. Local numerical model, deformed
Rys. 19. Lokalny model numeryczny, odkształcony

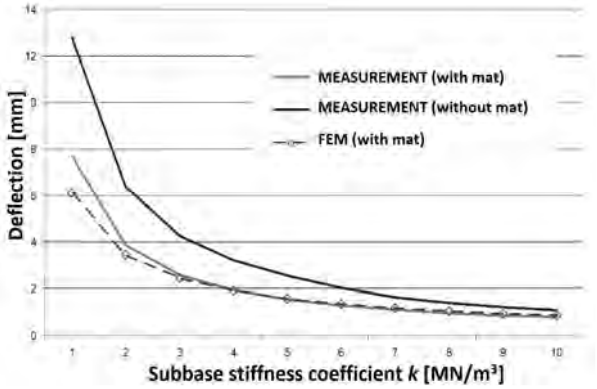

Fig. 20. Stiffness calibration results
Rys. 20. Wyniki kalibracji sztywności

The finite element simulation results for one of the braking variants are shown in Figure 21. A qualitative summary of the simulation results is shown in Figure 22, on which the normalized value of the measured reaction force obtained in the FEM analysis was 0.0578 N per each Newton of loading force, and the Von Mises stress amounted to 27.6 Pa per each Newton of loading force (in total, maximum stress computed amounted to 12.7 MPa in region of anchoring for load corresponding to full weight of truck).

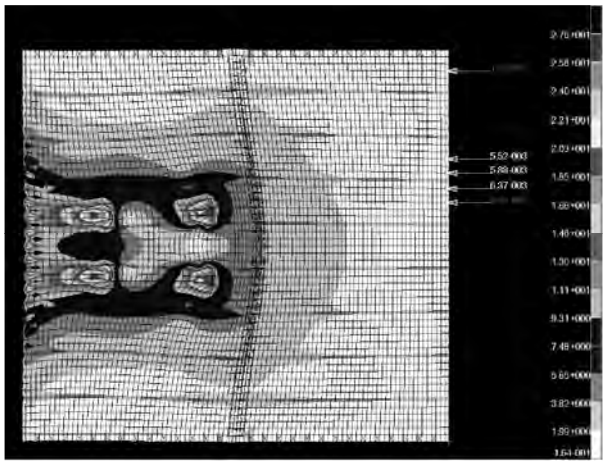

Fig. 21. FE analysis of resultant stress field
Rys. 21. Pole naprężeń uzyskane w symulacji

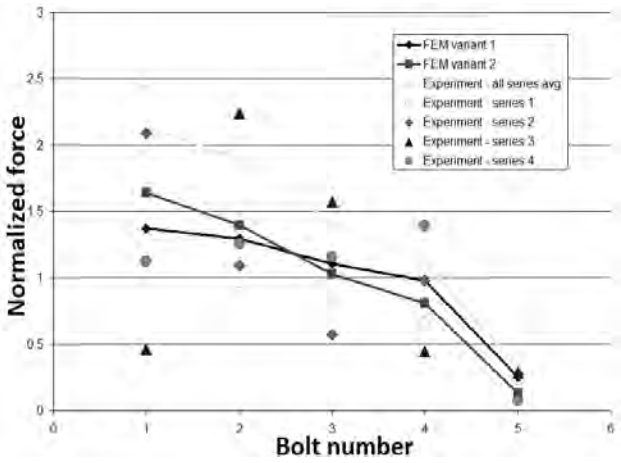

Fig. 22 Calculated reaction forces vs. experiment

Rys. 22. Porównanie wartości sił reakcji z eksperymentem

CONCLUSIONS

In the present paper, the results of the field and material tests, along with the results of a preliminary FEM analysis of the ELP-1 KRATER airfield mat are presented. In this paper, the anchoring region was considered to be the most critical area of the mat.

The results of static and dynamic tests show that the reaction forces in the anchoring bolts are considerably low, and for the heavy truck, noticeable load levels were recorded only for the most rapid and harsh braking maneuvers of a heavily laden truck whose mass was in the same order of magnitude as typical transport aircraft. The conservative finite element analysis results have confirmed these findings - it can be seen that the dominant mode of loading that may cause damage of the anchoring bolts results from frictional braking in-plane loads. The normal pressure loads determined in the numerical analysis act only in the immediate vicinity of the tire mark, and might contribute to abrasive wear of the mat - this factor was unaccounted for in the present paper. The following conclusions regarding the mat's operational regime and mechanical properties can be made:

1) The mat-subbase system which includes the mobile airfield mat and the newly formed crater filling is a sufficient supporting layer for loads induced by heavy vehicle loading.
2) Due to low recorded reaction force levels and low calculated stress levels, it can be concluded that the mobile composite airfield mat provides an adequate load bearing capacity for the aircraft and vehicles that utilize the mat
3) The foldable composite mat enables rapid pavement repair capabilities in the least possible amount of time, ensuring safe conditions for aircraft operations.
4) The low mass and ease of installation enable the composite mat to be used for a wide range of military and non-military tasks.

It should be noted that the high operational parameters of the Poland-manufactured airfield mat are comparable to the solutions utilized and manufactured worldwide.

REFERENCES

[1] STANAG 2929 (wydanie 2) - Naprawa Zniszczeń Lotniskowych, 1989.
[2] Dyrektywa Dowództwa Sojuszniczych Sił Zbrojnych NATO ACE 80-15, 1989.
[3] Wesołowski M., Pokrycie kompozytowe typu „KRATER" do odbudowy nawierzchni drogowych i lotniskowych w sytuacjach losowych, Nowoczesne technologie w budownictwie drogowym, Poznań 2009.
[4] Boczkowska A., Kapuściński J., Puciłowski K., Wojciechowski S., Kompozyty, WPW, Warszawa 2000.
[5] Nita P., Określenie wymagań fizyko-mechanicznych dla przenośnych pokryć lotniskowych, ITWL, Warszawa 2001.
[6] Nita P., Poświata A., Płyty kompozytowe przeznaczone na składane przenośne nawierzchnie lotniskowe, ITWL, Warszawa 2001.
[7] Wiłun Z., Zarys geotechniki, Wydawnictwo Komunikacji i Łączności, Warszawa 2001.
[8] ICAO, Aerodrome Design Manual Part 3, Pavements, Doc-9157-AN/901, 1983.
[9] Nita P., Budowa i utrzymanie nawierzchni lotniskowych, WKŁ, Warszawa 1999, 2008.
[10] Wesołowski M., Problemy nośności kompozytowych, mobilnych płyt nawierzchniowych, 56 Konferencja Naukowa Komitetu Inżynierii Lądowej i Wodnej PAN, Krynica 2010.
[11] Gonzalez C., Development of a New Design Methodology for Structural Airfield Mats, Transportation Research Board Annual Meeting 2009.
[12] Gartrell C.A., Full-Scale Instrumented Testing and Analysis of Matting Systems for Airfield Parking Ramps and Taxiways, 56 raport ERDC, Washington 2010.
[13] Wang W. et al., Jointed Plain Concrete Pavement Model Evaluation, Transportation Research Record, Journal of the Transportation Research Board, 2006.

